

Three-component model and tricritical points: A renormalization-group study. Two dimensions

Miron Kaufman and Robert B. Griffiths

Department of Physics, Carnegie-Mellon University, Pittsburgh, Pennsylvania 15213

Julia M. Yeomans and Michael E. Fisher

Baker Laboratory, Cornell University, Ithaca, New York 14853

(Received 21 October 1980)

The global phase diagram for a three-component lattice gas or spin-one Ising model with general single-site and nearest-neighbor "ferromagnetic" interactions is worked out for two-dimensional lattices using a Migdal-Kadanoff recursion relation. It differs in important qualitative respects from the corresponding mean-field phase diagram. The set of fixed points and flows provides the characteristic phase diagrams of the three-state Potts multicritical point and the ordinary ($n = 1$) tricritical point in a complete set of symmetry-breaking fields. The latter is associated, in this renormalization-group scheme, with seven distinct critical fixed points, a number which is surprisingly large.

I. INTRODUCTION

A spin-one model, in which each spin variable can take three values, is probably the simplest generalization of the ordinary spin- $\frac{1}{2}$ Ising model which can exhibit a variety of multicritical points without the necessity of breaking translational invariance (i.e., without "antiferromagnetism"). In lattice gas terminology, spin-one corresponds to three possible types of atoms (or two types plus vacuum) in each cell. Hence Furman *et al.*,¹ who worked out the complete global phase diagram for nearest-neighbor interactions in a mean-field approximation, have called this a "three-component model."

The mean-field approximation^{1,2} yields tricritical and fourth-order multicritical points³ in the "principal energy triangle," the range of parameters for which one does not have antiferromagnetic ground states. However, certain features of the mean-field phase diagram are not even qualitatively correct for a two-dimensional square lattice, which is the focus of the present study. In particular, a suitable choice of parameters in the Hamiltonian produces the three-state Potts model, which is known to have a continuous transition on this lattice,⁴ in contrast to the mean field and other classical theories which, for reasons pointed by Landau and Lifshitz,⁵ always yield a first-order transition.

Renormalization-group procedures can remedy the defect just mentioned, and previous authors have reported studies of a three-dimensional "even" subspace of the full five-dimensional field or parameter space of the three-component model on a square or triangular lattice using real-space or cell methods.⁶⁻⁹ In addition, Krinsky and Furman¹⁰ have studied a

one-dimensional model in the five-dimensional parameter space.

It should be stressed that a complete description of asymptotic tricriticality in nonsymmetric systems requires consideration of four parameters: two even fields and two odd fields.^{3,11} In this paper we extend the previous studies to the full parameter space for a two-dimensional lattice using a recursion scheme of the Migdal-Kadanoff type.¹² Several interesting results emerge from our study.

First, we have obtained the complete set of fixed points for the recursion relations in the space of five fields, and have thus determined the global phase diagram for the three-component model in two dimensions (in a renormalization-group approximation, of course). Second, we have obtained the complete characteristic phase diagrams, in the sense of Griffiths,^{3,11} for both the two-dimensional tricritical point and the three-state Potts point. For the former, the general topological characteristics are in agreement with classical theory, and the tricritical fixed-point exponents agree fairly well with previous estimates. The interesting feature which emerges is the manner in which the particular renormalization group studied produces the phase diagram through the structure of fixed points and flows. The result, Sec. VI, is remarkably complex, and could hardly have been anticipated without carrying out explicit calculations. In the case of the three-state Potts point it is, of course, impossible to obtain the characteristic phase diagram from a classical model, so another approach is essential. True enough, our results are not surprising in view of previous speculations,^{1,3} but it is nonetheless gratifying to see the anticipated answers emerge from an honest, albeit approximate, calculation.

An outline of the paper is as follows. After defining the model in Sec. II and describing the approximate recursion relations embodying the renormalization group in Sec. III, we list the fixed points and their exponents in Sec. IV. Section V contains a discussion of the global phase diagram and some features of the fixed point structure, while the tricritical points are the subject of Sec. VI. Conclusions and some open questions are presented in Sec. VII.

Whereas this paper is concerned almost entirely with the two-dimensional ($d=2$) square lattice, the same recursion relations can be applied in other dimensions as well. Various results from studying this dimensional dependence, together with a modification of the model which contains a free parameter which can be adjusted to yield good tricritical exponents for $d=2$, will be discussed in a future paper.

II. THREE-COMPONENT, OR SPIN-ONE, MODEL

The three-component model can be thought of as a lattice gas in which all of space is divided up into identical cells whose centers form the sites of a hypercubic (in two dimensions, a square) or perhaps some other lattice. Each cell is occupied by precisely one atom, which can be of one of three types: α , β , or γ . The projection operator P_i^α is 1 if the i th cell (centered at the i th lattice site) is occupied by an atom of type α , and is zero otherwise; P_i^β and P_i^γ are defined similarly. Note that

$$P_i^\alpha + P_i^\beta + P_i^\gamma = 1 \quad (2.1)$$

The total energy \mathcal{H} of a set of atoms has the form

$$-\frac{\mathcal{H}}{kT} = \sum_i (\bar{\mu}_\alpha P_i^\alpha + \bar{\mu}_\beta P_i^\beta + \bar{\mu}_\gamma P_i^\gamma) - q^{-1} \sum_{\langle ij \rangle} [\bar{a} (P_i^\beta P_j^\gamma + P_i^\gamma P_j^\beta) + \bar{b} (P_i^\alpha P_j^\gamma + P_i^\gamma P_j^\alpha) + \bar{c} (P_i^\alpha P_j^\beta + P_i^\beta P_j^\alpha)] \quad (2.2)$$

where T is the temperature, k is Boltzmann's constant, q is the coordination number of the lattice (4 for a square lattice), and $\langle ij \rangle$ denotes a nearest-neighbor pair of cells or sites, each pair occurring in the sum precisely once. The quantities

$$\zeta_a = e^{\bar{\mu}_a/\zeta}, \quad \zeta_b = e^{\bar{\mu}_b/\zeta}, \quad \zeta_c = e^{\bar{\mu}_c/\zeta} \quad (2.3)$$

with

$$\zeta = e^{\bar{\mu}_a} + e^{\bar{\mu}_b} + e^{\bar{\mu}_c} \quad (2.4)$$

sum up to unity, and serve as activities for the corresponding components. Note that ζ_a , ζ_b , and ζ_c depend only on the differences $\bar{\mu}_a - \bar{\mu}_c$, $\bar{\mu}_b - \bar{\mu}_c$. In fact, in view of the sum rule (2.1), the only effect of adding a constant to the $\bar{\mu}$'s is to add an uninteresting constant to \mathcal{H} .

In this paper we shall consider only the situation in which \bar{a} , \bar{b} , and \bar{c} are all non-negative. The reason is that a negative value of (say) \bar{a} , as is evident when (2.2) is exponentiated as a Boltzmann factor, tends to favor a situation in which neighboring cells are occupied by different types of atoms, and thus low-temperature states which lack translational invariance. It is doubtful whether such states and the associated phase diagrams will be described correctly by a simple recursion scheme of the sort introduced below in Sec. IV.

The lattice gas just described is equivalent to a spin-one Ising model in which the spin variable

$$s_i = P_i^\alpha - P_i^\beta \quad (2.5)$$

associated with the lattice site i takes the values 1, 0, or -1, and the energy \mathcal{H} has the form

$$-\frac{\mathcal{H}}{kT} = H \sum_i s_i - D \sum_i s_i^2 + q^{-1} \sum_{\langle ij \rangle} [J s_i s_j + K s_i^2 s_j^2 + \frac{1}{2} H_3 s_i s_j (s_i + s_j)] \quad (2.6)$$

The parameters appearing in (2.2) and (2.6) are related to one another in Table I, which also shows their

TABLE I. Correspondence between notations for various fields.

This paper Eq. (2.2)	This paper Eq. (2.6)	Furman, Dattagupta, and Griffiths ^a	Berker and Wortis ^b
\bar{a}	$\frac{1}{2}(J+K-H_3)$	\bar{a}	$\frac{1}{2}q(J+K-2L)$
\bar{b}	$\frac{1}{2}(J+K+H_3)$	\bar{b}	$\frac{1}{2}q(J+K+2L)$
\bar{c}	$2J$	\bar{c}	$2qJ$
$\frac{1}{2}(\bar{\mu}_a - \bar{\mu}_b)$	$H + \frac{1}{2}H_3$	$\frac{1}{2}(\nu_1 - \nu_2)$	$H + qL$
$\frac{1}{2}(\bar{\mu}_a + \bar{\mu}_b - 2\bar{\mu}_c)$	$-D + \frac{1}{2}(J+K)$	$\frac{1}{2}(\nu_1 + \nu_2)$	$-\Delta + \frac{1}{2}q(J+K)$

^aReference 1.

^bReference 6.

connection with variables appearing in some other papers. Note that J, K, H , etc. in (2.6) are equal to an energy divided by kT , in contrast to the convention employed in several previous papers^{1,2} devoted to this model.

Since only the differences between $\bar{\mu}$'s in (2.2) are physically relevant, $-\mathcal{H}/kT$ depends on five independent continuous real parameters or fields in both (2.2) and (2.6). This set is "complete" in the sense that it is the most general set of interactions involving only single sites and nearest-neighbors pairs which has the full symmetry of the lattice. As the Gibbs probability depends only on $-\mathcal{H}/kT$, the definition of temperature in terms of the parameters in (2.2) and (2.6) is somewhat arbitrary. We shall, for convenience, adopt the convention

$$T = (\bar{a} + \bar{b} + \bar{c})^{-1} = (K + 3J)^{-1} . \quad (2.7)$$

This agrees with Furman *et al.*¹ when \bar{a}, \bar{b} , and \bar{c} are all non-negative ("ferromagnetic"), which is the only case we shall consider. This definition makes T invariant under the permutations of a, b , and c discussed below. It is also convenient to introduce a normalized set of parameters, following Furman *et al.*,¹ namely,

$$\hat{a} = \bar{a}T, \quad \hat{b} = \bar{b}T, \quad \hat{c} = \bar{c}T , \quad (2.8)$$

whose sum is unity

$$\hat{a} + \hat{b} + \hat{c} = 1 . \quad (2.9)$$

An important symmetry of (2.2) is connected with permutations of the particle labels, α, β, γ . For example, \mathcal{H}/kT is unchanged if the permutation $\alpha \Rightarrow \beta \Rightarrow \gamma \Rightarrow \alpha$, which we denote as usual by $(\alpha\beta\gamma)$, is accompanied by a simultaneous permutation (abc) applied *both* to the "energy parameters" \bar{a}, \bar{b} , and \bar{c} , and to the "chemical potentials" $\bar{\mu}_a, \bar{\mu}_b, \bar{\mu}_c$. In addition, there are certain subspaces of the space of the five fields \bar{a}, \bar{b} , etc. which are invariant under all or some of the permutations of a, b , and c (in the sense just described). The one-dimensional space

$$\bar{a} = \bar{b} = \bar{c}, \quad \bar{\mu}_a = \bar{\mu}_b = \bar{\mu}_c \quad (2.10a)$$

corresponding to

$$H = H_3 = 0, \quad K = 3J, \quad D = 2J \quad (2.10b)$$

is invariant under all permutations, and corresponds to the standard three-state Potts model with temperature as the only variable. It might be called the "Potts space." The three-dimensional space

$$\bar{a} = \bar{b}, \quad \bar{\mu}_a = \bar{\mu}_b \quad (2.11a)$$

corresponding to

$$H = H_3 = 0 \quad (2.11b)$$

is invariant under (ab) . There are two other analo-

gous subspaces, one invariant under (bc) and the other under (ac) . They may be termed the "even spaces" since the corresponding odd fields vanish identically for the space defined by (2.11).

III. RECURSION RELATIONS

We have employed a Migdal-Kadanoff¹² type of approximate renormalization group which derives recursion relations in two steps: (i) bond moving followed by (ii) one-dimensional (exact) decimation. These steps are illustrated in Fig. 1 for the case we have employed, in which the spatial rescaling factor b is equal to 2. In step (i) the single-site energies ($\bar{\mu}_a$, etc.) are divided evenly among the bonds incident at the site and are then moved with the bonds,¹³ a procedure which yields exact results for ground-state energies and hence a correct "anchor" at $T=0$. The transformation produced by these two steps maps the parameter space (\bar{a}, \bar{b} , etc.) onto itself. It is important to note that this mapping commutes with all the permutation operations discussed in Sec. II, and thus preserves the various symmetries of the problem. In particular, the Potts space (2.10) and the even spaces (2.11) are mapped onto themselves. In addition the transformation maps the space

$$\bar{a} = \bar{b}, \quad \bar{c} = 0 \quad (3.1a)$$

(see Appendix A) or, equivalently,

$$H_3 = J = 0 \quad (3.1b)$$

onto itself.

The explicit recursion formulas are

$$w'_a = \frac{(\zeta_a^p w_b w_c + \zeta_b^p w_a + \zeta_c^p w_a)^r}{(\zeta_a^p w_b^2 + \zeta_b^p w_a^2 + \zeta_c^p)^{r/2} (\zeta_a^p w_c^2 + \zeta_b^p + \zeta_c^p w_a^2)^{r/2}} , \quad (3.2)$$

$$\zeta'_a = C \zeta_a^r (\zeta_a^p + \zeta_b^p w_c^2 + \zeta_c^p w_b^2)^{r/p} , \quad (3.3)$$

and a corresponding set of equations for w'_b, w'_c, ζ'_b ,

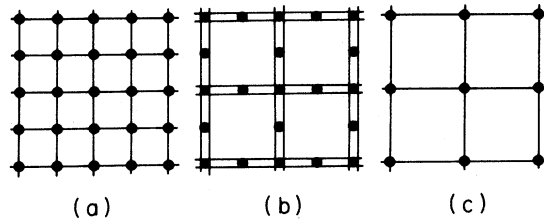


FIG. 1. Migdal-Kadanoff recursion scheme. Starting with (a), bonds (together with single-site interactions) are shifted to produce the pattern in (b). The spins with only two neighbors are then summed out to produce the new set of nearest-neighbor interactions indicated in (c).

and ζ'_c obtained by permuting a , b , and c on both sides of (3.2) and (3.3). Here we have

$$w_a = \exp(-p\bar{a}/2) , \quad (3.4)$$

with w_b and w_c defined in a corresponding manner. The constants

$$p = 2^d/q, \quad r = 2^{d-1} \quad (3.5)$$

are equal to 1 and 2, respectively, for a square lattice ($d=2, q=4$). The constant, C , on the right-hand side of (3.3) is adjusted for each iteration so that $\zeta'_a + \zeta'_b + \zeta'_c$ is maintained equal to unity [see (2.4)].

It has been pointed out by Berker and Ostlund¹⁴ that the recursion scheme described above, while it is approximate for a square (or hypercubic, etc.) lattice, is actually an exact renormalization-group transformation for a certain class of models on lattices which possess a hierarchical structure but lack translational invariance. This fact is of some interest in connection with certain "anomalies" to be discussed below. However it also serves to guard against nonphysical results, such as negative specific heats, to which approximations are prone.

There are alternative Migdal-Kadanoff schemes which differ from that described above. One consists in reversing the order of steps (i) and (ii) above. The difference in terms of flows and fixed points between this scheme and the one we have used is rather trivial: our fixed point values for a $\bar{\mu}_a$, etc. are simply multiplied by a factor of b^{d-1} , but the exponents are identical. On the other hand, if the one-site interactions are *not* moved with the bonds, as in the scheme of Emery and Swendsen¹⁵ (see Appendix A), the results differ in several notable respects from the scheme we have used.

IV. FIXED POINTS AND CRITICAL EXPONENTS

The fixed points of the recursion relations presented in Sec. III for the case $d=2$ are listed in Table II, and the corresponding exponents are given in Table III. Following Furman *et al.*,¹ we use symbols A^2 ($=AA$) and A^3 to denote points of two- or three-phase coexistence, respectively, or the corresponding manifolds in a phase diagram, and B , BA , and C for critical points, critical end points, and tricritical points. The symbol Y , suggesting threefold symmetry, denotes a three-state Potts multicritical point. Fixed points corresponding to any of these thermodynamic entities are denoted by placing the symbol for the entity in angular brackets, e.g., $\langle BA \rangle$ denotes a fixed point describing a simple critical end point, and using subscripts, and occasionally superscripts, to differentiate different fixed points corresponding to the same entity.

Because the recursion relations preserve the per-

mutation symmetries, the fixed points occur in equivalence classes in which the different points are images of each other under the permutation operations on a , b , and c as described in Sec. II. In Table II we list only one example from each equivalence class, while the number of members in the equivalence class, m , is indicated in the second column. The symbols for the other fixed points in the same class can be obtained by applying appropriate permutations of α , β , and γ to the *subscripts* associated with the symbol in the table, and *simultaneously* the corresponding permutation of a , b , and c to *both* the $\bar{a}, \bar{b}, \bar{c}$ columns and the $\zeta_a, \zeta_b, \zeta_c$ columns of the table. For example, Table II gives parameter values for the critical fixed point $\langle B \rangle_{\gamma\alpha}$ and notes that there are six fixed points in this equivalence class: the symbols for the other five are: $\langle B \rangle_{\gamma\beta}$, $\langle B \rangle_{\alpha\beta}$, $\langle B \rangle_{\alpha\gamma}$, $\langle B \rangle_{\beta\alpha}$, and $\langle B \rangle_{\beta\gamma}$. To obtain the parameter values for $\langle B \rangle_{\beta\gamma}$ from those given for $\langle B \rangle_{\gamma\alpha}$, we note that the permutation $(\alpha\gamma\beta)$ applied separately to each of the subscripts, γ and α , of the latter yields the subscripts, β and γ of the former. The corresponding permutation of a , b , and c is (acb) . Hence the parameters for $\langle B \rangle_{\beta\gamma}$ are obtained by taking the number in column \bar{a} opposite $\langle B \rangle_{\gamma\alpha}$ in the table and moving it to \bar{c} , the number in \bar{c} to \bar{b} , etc., and also the number in column ζ_a to ζ_c , etc. A similar process is applied in the case of fixed points carrying only one subscript. For example, the parameters for $\langle B \rangle_{\beta}^0$ can be obtained from those listed for $\langle B \rangle_{\gamma}^0$ by applying (bc) [or (acb)] to the numbers in the two sets of columns, as just described.

In the case of A^2 and A^3 , the recursion relations result in families of fixed points described by one and two continuous parameters, respectively. For $\langle A^2 \rangle$, we have broken the family down into three separate sets, as indicated in Table II; in order to distinguish some of the flows (Table IV). Presumably a similar decomposition is possible for $\langle A^3 \rangle$, but we have not attempted to carry it out. The infinite temperature fixed points are denoted by $\langle A \rangle$, consistent with other notation, and $\langle A \rangle_0$ is invariant under all permutations. We have no proof that we have found all the fixed points, but various lines of evidence suggest that the set listed in Table II is complete.

The renormalization-group exponents y_i (sometimes denoted by λ_i) associated with different fixed points and listed in Table III are defined by

$$y_i = \ln \Lambda_i / \ln b , \quad (4.1)$$

where Λ_i is one of the eigenvalues of the recursion relations of Sec. III linearized about the fixed point, and $b=2$ in our case. Since all fixed points in an equivalence class have precisely the same exponents, only one example of each is given in Table III. For fixed points in the invariant even space (2.11), i.e., those carrying a single subscript γ , the exponents have been separated into two sets, even (y_2, y_4, y_6)

TABLE II. Fixed points of the approximate recursion relations for $d = 2, q = 4$.

Label	m	ζ_a	ζ_b	ζ_c	\bar{a}/q	\bar{b}/q	\bar{c}/q	qT^a
$\langle Y \rangle$	1	$\frac{1}{3}$	$\frac{1}{3}$	$\frac{1}{3}$	0.693 15	0.693 15	0.693 15	0.4809
$\langle C \rangle_\gamma$	3	0.342 3	0.342 3	0.3160	0.539 2	0.539 2	2.085 9	0.3160
$\langle B \rangle_\gamma^0$	3	0.282 1	0.282 1	0.4358	0.618 0	0.618 0	0	0.8090
$\langle B \rangle_\gamma$	3	$\frac{1}{2}$	$\frac{1}{2}$	0	0.129 5	0.129 5	0.609 4	1.1515
$\langle B \rangle_{\gamma\alpha}$	6	$\frac{1}{2}$	$\frac{1}{2}$	0	0	0.609 4	0.609 4	0.8205
$\langle BA \rangle_\gamma$	3	0.327 05	0.327 05	0.3459	∞^b	∞^b	0.609 4	0
$\langle BA \rangle_{\gamma\alpha}$	6	0.327 05	0.327 05	0.3459	∞^c	∞^c	0.609 4	0
$\langle A^3 \rangle$	1	$\frac{1}{3}$	$\frac{1}{3}$	$\frac{1}{3}$	∞^d	∞^d	∞^d	0
$\langle A^2 \rangle_\gamma^0$	3	0.278 75	0.278 75	0.4425	∞^b	∞^b	0	0
$\langle A^2 \rangle_\gamma$	3	$\frac{1}{2}$	$\frac{1}{2}$	0	$\frac{1}{2} \ln 2$	$\frac{1}{2} \ln 2$	∞^e	0
					∞^f	0	∞^f	
					0	∞^g	∞^g	
$\langle A \rangle_0$	1	$\frac{1}{3}$	$\frac{1}{3}$	$\frac{1}{3}$	0 ^h	0	0	∞
$\langle A \rangle_\gamma$	3	$\frac{1}{2}$	$\frac{1}{2}$	0	0 ^h	0	0	∞
$\langle A \rangle_\gamma^0$	3	0	0	1	0 ^h	0	0	∞

^aSee Eq. (2.7).

^b $\bar{a} = \bar{b}, \hat{a} = \hat{b} = \frac{1}{2}$.

^c $\bar{a} = 1.7556q + \bar{b}, \hat{a} = \hat{b} = \frac{1}{2}$.

^d $\hat{a} \leq \frac{1}{2}, \hat{b} \leq \frac{1}{2}, \hat{c} \leq \frac{1}{2}, \hat{a} + \hat{b} + \hat{c} = 1$.

^e $\hat{c} = 1$.

^f $\hat{a} \leq \frac{1}{2}, \hat{c} \geq \frac{1}{2}, \hat{a} + \hat{c} = 1$.

^g $\hat{b} \leq \frac{1}{2}, \hat{c} \geq \frac{1}{2}, \hat{b} + \hat{c} = 1$.

^h $\hat{a}, \hat{b}, \hat{c} \geq 0$ and $\hat{a} + \hat{b} + \hat{c} = 1$.

TABLE III. Exponents of the various fixed points listed in Table II [see Eq. (4.1)].

Label	Codimension	ν_2	ν_4	ν_6	ν_1	ν_3
$\langle Y \rangle$	5	0.8299			1.8679 ^a	0.5472 ^a
$\langle C \rangle_\gamma$	4	1.7734	0.5186	-1.2905	1.9365	0.8108
$\langle B \rangle_\gamma^0$	3	0.7550	1.8773	$-\infty$	1 ^b	-0.4160
$\langle B \rangle_\gamma$	3	0.7473	$-\infty$	$-\infty$	1.8792	0.1209
$\langle B \rangle_{\gamma\alpha}$	2	0.7473	$-\infty$	$-\infty$	1.8792	-0.2527
$\langle BA \rangle_\gamma$	4	0.7473	2(=d)	$-\infty$	1.8792	0.5827
$\langle BA \rangle_{\gamma\alpha}$	3	0.7473	2(=d)	$-\infty$	1.8792	-1.5752

^aThese exponents are doubly degenerate; see text.

^bThe Migdal-Kadanoff scheme predicts $\nu_1 = d - 1$ for all dimensions.

TABLE IV. Summary of renormalization-group flows linking the various fixed points.

$\langle Y \rangle$	$\langle C \rangle_\alpha, \langle C \rangle_\beta, \langle C \rangle_\gamma, \langle BA \rangle_\alpha, \langle BA \rangle_\beta, \langle BA \rangle_\gamma$
$\langle C \rangle_\gamma$	$\langle BA \rangle_{\alpha\gamma}, \langle BA \rangle_{\beta\gamma}, \langle B \rangle_\alpha^0, \langle B \rangle_\beta^0, \langle B \rangle_\gamma$
$\langle BA \rangle_\gamma$	$\langle BA \rangle_{\gamma\alpha}, \langle BA \rangle_{\gamma\beta}, \langle B \rangle_\gamma$
$\langle BA \rangle_{\gamma\alpha}$	$\langle B \rangle_{\gamma\beta}, \langle A^3 \rangle, \langle A^2 \rangle_\gamma^0$
$\langle B \rangle_\gamma^0$	$\langle B \rangle_{\alpha\gamma}, \langle B \rangle_{\beta\gamma}, \langle A^2 \rangle_\gamma^0, \langle A \rangle_0$
$\langle B \rangle_\gamma$	$\langle B \rangle_{\gamma\alpha}, \langle B \rangle_{\gamma\beta}$
$\langle B \rangle_{\gamma\alpha}$	$\langle A^2 \rangle_\gamma, \langle A \rangle_\gamma$
$\langle A^3 \rangle$	$\langle A^2 \rangle_\alpha, \langle A^2 \rangle_\beta, \langle A^2 \rangle_\gamma$
$\langle A^2 \rangle_\gamma^0$	$\langle A^2 \rangle_\alpha, \langle A^2 \rangle_\beta, \langle A \rangle_\gamma$
$\langle A^2 \rangle_\gamma$	$\langle A \rangle_\alpha^0, \langle A \rangle_\beta^0$
$\langle A \rangle_0$	$\langle A \rangle_\alpha, \langle A \rangle_\beta, \langle A \rangle_\gamma$
$\langle A \rangle_\gamma$	$\langle A \rangle_\alpha^0, \langle A \rangle_\beta^0$

and odd (y_1, y_3) corresponding to eigenfunctions belonging to the even and odd irreducible representations of the group $\{(ab), E\}$. In the language appropriate to a Landau or classical descriptions of tricriticality^{3,12} the odd eigenvalues correspond to the odd fields coupling to s and s^3 , where s is the scalar order parameter, while the even ones correspond to the fields coupling to s^2, s^4 , and s^6 . In the case of the Potts fixed point, $\langle Y \rangle$, the “even” exponents correspond to the identity and the “odd” exponents to the two-dimensional irreducible representations of the permutations of a, b , and c ; naturally, the “odd” exponents are twofold degenerate. In the language of a two-component order parameter $\vec{s} \equiv (s_x, s_y)$ the odd eigenvalues include those of the ordering field \bar{h} coupling directly to \vec{s} . For fixed points which are not in invariant subspaces, the exponents are listed in a manner corresponding to their more symmetrical counterparts.

The leading odd or “magnetic” and even or “thermal” exponents for $\langle B \rangle$ and $\langle BA \rangle$ in Table III may be compared with the exact results¹⁶ $y_1 = \frac{15}{8} = 1.875$ (note that this corresponds to y_4 for $\langle B \rangle_\gamma^0$) and $y_2 = 1$ for ordinary Ising critical points in two dimensions. For the Potts point $\langle Y \rangle$ and the tricritical points $\langle C \rangle$, exact values are not known. However, there is a plausible conjecture¹⁷ that $y_1 = \frac{28}{15} = 1.8667$, $y_2 = \frac{6}{5} = 1.200$ for $\langle Y \rangle$ and $y_1 = \frac{28}{40} = 1.925$, $y_2 = \frac{7}{5} = 1.800$ for $\langle C \rangle$.

At the $\langle A^2 \rangle$ and $\langle BA \rangle$ fixed points there is an eigenvalue exactly equal to d , while at $\langle A^3 \rangle$ there are two exponents equal to d , in accordance with what

one would expect for phase coexistence.¹⁸ In addition, as one would expect, y_1 and y_2 at the $\langle BA \rangle$ fixed points agree with the values for $\langle B \rangle_\gamma$. That these desirable features should be reproduced by the Migdal-Kadanoff approximate renormalization scheme is not *a priori* clear, but the observation of Berker and Ostlund that the recursion relations are realizable on a definite, if unusual, model makes the result somewhat less surprising.

Table III also shows the codimensions of the manifolds which flow into (and are thus “governed” by) the various fixed points. We remind the reader that in the usual renormalization-group phenomenology, the manifold governed by the fixed point is (typically) in the same universality class as the fixed point. The codimension of this manifold (the dimension of the parameter space less the dimension of the manifold) is equal to the number of positive exponents at the fixed point and hence to the number of relevant scaling fields. However, the manifolds governed by various fixed points of the same type, e.g., $\langle B \rangle$ or $\langle BA \rangle$, may be part of a larger smooth thermodynamic manifold of a particular type. In this case the codimension of the former may be greater than the codimension of the latter; i.e., the dimension of the manifold governed by a particular fixed point can be less than that of the thermodynamic manifold of which it is a part. This feature of the renormalization-group flows will be discussed further below.

The renormalization-group flows linking the fixed points are summarized in Table IV, using the following convention. From the immediate vicinity of a fixed point listed in the first column there are flows to all of the fixed points listed in the second column, and *also* to *all* fixed points which can be reached by

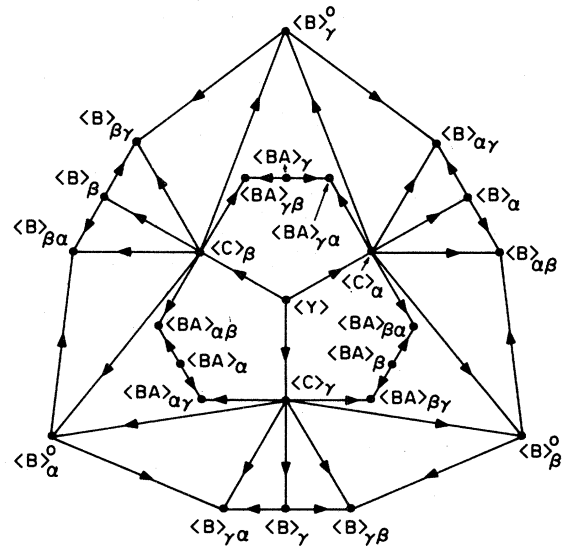


FIG. 2. Schematic diagram showing a selected set of fixed points and some of the interconnecting flows.

flows from the latter. Thus, for example, there is a flow from $\langle C \rangle_\gamma$ to $\langle A^2 \rangle_\gamma$ even though the latter is not explicitly listed in the second column opposite $\langle C \rangle_\gamma$ in the first. Once again, only one member of an equivalence class is listed in the first column, since flows for the other members can be determined quite easily using symmetry.

Due to the high dimensionality of the parameter space and the large number of fixed points, it is not very helpful to present all of the fixed points and flows on a single diagram. A selected set of fixed points are shown in a schematic projection in Fig. 2, which clearly shows the threefold symmetry associated with the Potts, tricritical, and various critical fixed points. We turn now to a discussion of this figure and other features of interest.

V. SOME PROPERTIES OF THE FIXED POINTS AND PHASE DIAGRAMS

A. Critical fixed points

The critical fixed points $\langle B \rangle$ listed in Tables II to IV and displayed in Fig. 2 show a number of interesting features. First, it is worth noting that $\langle B \rangle_{\gamma\beta}$ and $\langle B \rangle_{\gamma\alpha}$ can be regarded as "satellites" of $\langle B \rangle_\gamma$. Not only are the exponents the same (with one exception), but also these three fixed points in a sense represent identical physical situations. In particular, the extra relevant eigenvalue associated with $\langle B \rangle_\gamma$, corresponding to a flow outwards to the two satellites, does *not* mean that $\langle B \rangle_\gamma$ is in a separate universality class from $\langle B \rangle_{\gamma\alpha}$. Further details regarding this situation will be found in Appendix B. Of course both $\langle B \rangle_\alpha$ and $\langle B \rangle_\beta$ possess a corresponding set of satellites to which the same discussion applies.

By contrast, the critical points $\langle B \rangle_\gamma$ and $\langle B \rangle_\gamma^0$ have exponents which are slightly different. Both fixed points occur within the invariant even space (2.11), yet within this space they play different roles. The first, $\langle B \rangle_\gamma$, is an attractor for critical points corresponding to symmetry-breaking phase transitions at which $\langle S_i \rangle$ acquires a nonzero value despite the fact that $H = H_3 = 0$ in the spin representation (2.6). On the other hand, $\langle B \rangle_\gamma^0$ is a sink for critical points bounding first-order phase transitions across which, $\langle S_i^2 \rangle$ is discontinuous, but no symmetries of the Hamiltonian are broken.

The difference in the exponents between $\langle B \rangle_\gamma$ and $\langle B \rangle_\gamma^0$ must be regarded as a defect if one regards this renormalization group as an approximation for describing the model (2.2) on a square (or hypercubic) lattice, for one can show quite rigorously (see Appendix A) that the corresponding critical points should have the same Ising-like properties. On the other hand, one may (as noted in Sec. III) regard the

renormalization group as providing an exact solution for a particular model which lacks the usual translational symmetry. Viewed from the perspective just mentioned, one can regard $\langle B \rangle_\gamma^0$ as corresponding to some special sort of multicritical point. Unfortunately, the theory of infinite systems lacking normal translational invariance is not very well understood, so it is hard to say anything more about the possible character of such points and its significance, if any, for more realistic systems.

B. Global phase diagram

The fixed points and flows described in Sec. III serve to determine the global phase diagram of the three-component model in what Furman *et al.*¹ termed the "principal energy triangle," defined by \bar{a} , \bar{b} , and \bar{c} all non-negative, which is equivalent to $J \geq 0$, $J + K \geq |H_3|$. (When these parameters become negative one expects antiferromagnetism at low temperatures, and the bond-shifting recursion relations we have employed are not expected to give physically meaningful results under such circumstances.) This diagram differs from that obtained in the mean-field theory in two significant *qualitative* aspects. In the first place, the "shield" region which Furman *et al.* identified near the center of the principal energy triangle has completely disappeared. This is not surprising, since the existence of such a region is closely connected with the first-order nature of the transition predicted for the three-state Potts model in a classical theory, whereas our renormalization-group approach (in agreement with exact results for $d = 2$) predicts a continuous transition. Thus at the center of the principal energy triangle we find a simple situation, Fig. 3, in which three lines of tricritical points meet at the three-state Potts point. [This may be contrasted with Fig. 3(b) of Ref. 1.]

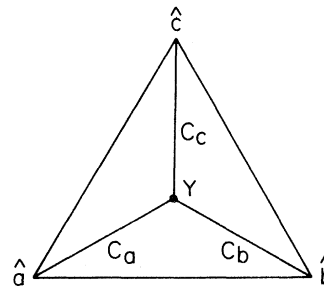


FIG. 3. Projection of the phase diagram on the principal energy triangle (the coordinate of a point is the center of mass if weights proportional to \hat{a} , \hat{b} , and \hat{c} are placed at the corresponding vertices). There are three lines of tricritical points (C_a, C_b, C_c) which meet at the three-state Potts point at the center of the diagram.

TABLE V. Estimates of the tricritical coordinates for $K = 0$ on the square and triangular lattice.

Lattice	Field	This paper	Mean field ^a	Monte Carlo ^b		Renormalization group	
Square	D	2.1	$2 \ln 2 \approx 1.4$	2.8	2.5	3.4 ^c	
	J/q	1.1	$\frac{3}{4}$	1.5	1.3	1.7 ^c	
Triangular	D	3.1	$2 \ln 2 \approx 1.4$			1.8 ^d	2.6 ^e
	J/q	1.1	$\frac{1}{2}$			0.67 ^d	1.0 ^e

^aReference 2.

^bMonte Carlo simulations for a 60×60 (first column, Ref. 22) and a 100×100 (second column, Ref. 23) array. The simulations probably give values of the parameters which are too small (private communication from D. P. Landau).

^cReferences 6 and 7.

^dReference 8.

^eReference 9.

The other feature which is qualitatively different from mean-field predictions is that the lines of tricritical points extend out to the vertices of the principal energy triangle, as shown in Fig. 3, and are not interrupted, in their course outwards from the center, by the fourth-order points which occur in mean-field theory (see Fig. 3 of Furman *et al.*¹). Since mean-field theory makes predictions which are qualitatively incorrect near the center of the principal energy triangle for $d = 2$, it is perhaps not surprising if it fails to give qualitatively correct answers elsewhere, as well. However, it is perhaps worth adding the caution that real-space renormalization-group methods are also quite capable of giving qualitatively misleading answers (as, for instance, in the case of q -state Potts models for $q \geq 5$, prior to the recent work of Nienhuis *et al.*¹⁹). Hence, although we are inclined to favor the diagram in Fig. 3 as qualitatively correct for $d = 2$, some doubt must remain until it has been confirmed by other procedures.

In terms of the various thermodynamic manifolds which occur in the principle energy triangle, we predict a three-state Potts point Y of codimension 5, and, in addition, the following subset of the manifolds described by Furman *et al.*¹ (see their Tables II and IV): tricritical C_a, C_b, C_c , critical end points $(BA)_a, (BA)_b, (BA)_\gamma$, critical B , and first order A^3 and A^2 . Note that in the case of B, A^3 , and A^2 , we expect only one smooth manifold (for each entity) in the principal energy triangle. This is, of course, not inconsistent with the renormalization-group flows having several different fixed points governing the different parts of the same manifold (but see the discussion of $\langle B \rangle_\gamma^0$ in Appendix A).

The characteristic phase diagram³ for the three-state Potts point, Y , is simply that part of the global phase diagram which occurs in the immediate vicinity of this point. It is evident from Tables III and IV

that in the five-dimensional space, Y is connected to three distinct lines of tricritical points C , and each pair of lines is joined by a two-dimensional surface of critical end points BA (note that the satellite fixed points $\langle BA \rangle_{\gamma\alpha}$ and $\langle BA \rangle_{\gamma\beta}$ are really physically indistinguishable from $\langle BA \rangle_\gamma$). The remaining entities, B, A^3, A^2 , and A , all occur on single, connected manifolds of appropriate codimension.

In terms of actual numerical results for the locations of different entities, our Migdal-Kadanoff recursion scheme is not particularly accurate. The values of J for $\langle B \rangle_\gamma$ and $\langle Y \rangle$, and of K for $\langle B \rangle_\gamma^0$ are smaller than the corresponding exact results^{16,20,21} by about 30%. Interestingly enough, the ratios of our renormalization-group values to the exact results for these quantities are almost identical (the average ratio is 0.69) in all three cases, varying by less than 2%. The location of the Blume-Capel tricritical point in the invariant even space (2.11) at $K = 0$ has been estimated previously by several different methods,^{2,6-9,22,23} and the results are shown in Table V along with the values (for a square and triangular lattice) given by the present recursion relations. Again, the present results, while a considerable improvement on mean-field theory, do not seem very accurate.

VI. TRICRITICAL POINTS

The classical theory of tricritical points described by a single order parameter, of the type one expects in an Ising model or in an ordinary fluid mixture, predicts a codimension of 4. This means that four thermodynamic field variables are needed to describe the characteristic phase diagram^{3,11} near a tricritical point, and that additional field variables will simply produce lines or surfaces, etc., of tricritical points.

Our result showing four relevant eigenvalues (positive y_i , Table III) is in accord with this expectation and with previous real-space renormalization-group calculations. In addition, however, the fixed points and flows of Tables II and IV provide a description of the characteristic four-dimensional phase diagram for a tricritical point, which has not previously (so far as we know) been obtained using renormalization-group methods.

The manifold of critical points inside a small ball centered at a tricritical point in a space of four fields is expected, from the classical theory, to resemble a two-dimensional disk, see Fig. 4(a), with a cut running from the periphery (where the manifold leaves the ball) to the center.²⁴ Each edge of the cut is a line of critical end points, and these two lines meet in a cusp at the center of the disk, i.e., at the tricritical point. This "cut disk" picture appears in an interesting way in terms of the fixed points and flows near a single tricritical fixed point in our renormalization-group analysis, as indicated schematically in Fig. 4(b). Not unexpectedly, there are two separate critical end-point (BA) fixed points, one for each of the manifolds constituting the edges of the cut. However, the multiplicity of critical (B) fixed points is something of a surprise. There seems to be no good reason why a single critical fixed point should not suffice, as illustrated in Fig. 4(c), and it is an interesting question why so many actually occur in the present renormalization group. The existence of the satellites of $\langle B \rangle_\gamma$, may perhaps be related to the fact that this fixed point occurs with the field D , in (2.6), equal to $-\infty$. On the other hand, it is not clear why $\langle B \rangle_\alpha^0$ and $\langle B \rangle_\beta^0$ should play an essential role near $\langle C \rangle_\gamma$. It may be that the threefold symmetry of the global phase diagram (see Fig. 2) imposes certain constraints on the flows, and leads in some natural way to the large number of critical fixed points shown in Fig. 4(b).

Yet another way of viewing the renormalization-group flows for a tricritical point may be helpful. In Fig. 5(a) we have sketched the phase diagram near a tricritical point in the three-dimensional T, DT, HT space, showing the "wing" critical lines diverging from the tricritical point. Also indicated are the fixed points which govern the manifolds which include the critical and tricritical points. (The reader must resist the temptation of supposing that the flows to the critical fixed points actually take place *along* the critical lines in this diagram, since this is *not*, in general, the case.) In the case of a tricritical point in an n -vector model with $n \geq 2$, the wing critical points will belong to a different universality class (namely $n = 1$ or Ising-like) from those in the symmetry plane $H = 0$.¹¹ It would be quite impossible to describe this situation by the simple fixed point structure suggested in Fig. 4(c). It would still seem, however, that a structure less complicated than in Fig. 4(b), say one with only three critical fixed points, would suffice in a natural way.

For $H_3 < 0$, Fig. 5(b) replaces Fig. 5(a) as a schematic phase diagram in the T, DT, HT space: note that the tricritical point is replaced by a single critical point. Again, the fixed points governing the different critical manifolds are indicated. In this case there is no longer any flow to $\langle B \rangle_\gamma$, which lies in the even space. The continuous line of critical points, all of which are expected (on physical grounds) to be Ising-like, can be divided into two segments. One of these, which includes the portion with $DT < 0$, flows to $\langle B \rangle_{\gamma\beta}$, and the other flows to $\langle B \rangle_{\alpha\beta}$. The point which separates these two segments flows to $\langle B \rangle_\beta^0$ and is on a smooth extrapolation (the dashed line in the figure) of the three-phase line. As explained above, the eigenvalues of $\langle B \rangle_\beta^0$ and $\langle B \rangle_{\gamma\beta}$ are not precisely equal, so that within our approximation this point on the critical line has distinct exponents (see Appendix A). The dashed line, together with the

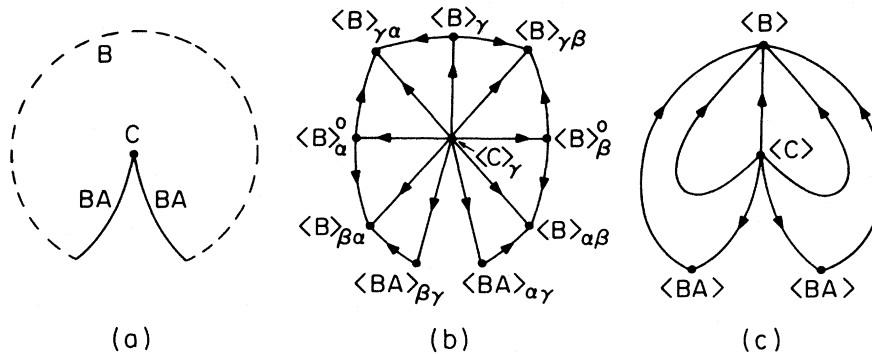


FIG. 4. (a) Topology of the critical surface near a tricritical point (see text). (b) The topology of fixed points and flows near a tricritical fixed point in the Migdal-Kadanoff scheme. (c) A hypothetical minimal set of fixed points and flows near a tricritical point.

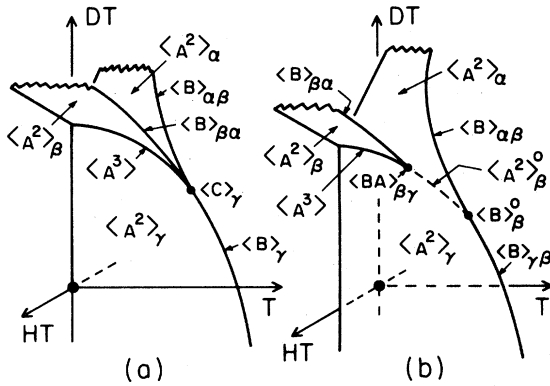


FIG. 5. Coexistence surfaces and critical lines (schematic) in the T, HT, DT , space for (a) $H_3=0$ and (b) H_3T negative. The fixed points governing the different manifolds are as indicated.

three-phase line, divides the main coexistence surface into two regions, one flowing to $\langle A^2 \rangle_\gamma$ and the other to $\langle A^2 \rangle_\alpha$, whereas the dashed line itself flows to $\langle A^2 \rangle_\beta^0$. Thanks to the fact that all of these fixed points have an eigenvalue equal to $d(=2)$, as noted above, they all correctly describe first-order transitions.

VII. CONCLUSIONS

The principal conclusions of our study are two in number, and each of them is connected with some interesting problems, regarding both the model and renormalization-group methods, which can only be answered by further study.

First, the global phase diagram for the three-component model in two dimensions, within the principal energy triangle ($\bar{a}, \bar{b}, \bar{c} \geq 0$ or $J \geq 0$, $J + K \geq |H_3|$) appears to have a remarkably simple form, especially when compared with the mean-field results of Furman *et al.*¹ In the five-dimensional field space one finds a three-state Potts multicritical point connected to three lines of tricritical points, Fig. 3, and then the minimal set of critical end-point manifolds which one might have anticipated under this circumstance. The "shield" region of the mean-field theory disappears, and we also find no trace of the fourth-order points, double critical points (B^2), etc. which are present in the classical global phase diagram. Is the renormalization-group result really reliable for $d=2$? And assuming that it is, at what dimensionality do the various classical features reappear? The answers to these questions must await further study.

That part of the global phase diagram which is near the three-state Potts point is what one believes to be

the characteristic five-dimensional diagram for this entity. While present evidence suggests that this type of multicritical point does not occur in three-dimensional systems, it is not inconceivable that at some future date experimental studies of two-dimensional systems will yield sufficient data to check our predictions.

Second, the renormalization-group we have employed produces the expected classical phase diagram near a tricritical point (with, of course, nonclassical exponents) by means of flows to two critical end-point fixed points, as one might have expected, and a total of *seven* critical fixed points, many more than seem (intuitively, at least) necessary in order to produce the desired result. To be sure, two of the extra fixed points are off-symmetry "satellites" which seem, in some sense, physically equivalent to a fixed point in the same invariant space as the tricritical point. We are, however, not sure whether they are necessary in all renormalization-group schemes. It would be of interest to see if one could produce a renormalization group which could produce the global phase diagram near a tricritical point using a smaller set of critical fixed points. Does one really need more than the single point shown in Fig. 4(c)? The answer is not obvious. In terms of the set of fixed points which actually occur in our Migdal-Kadanoff approximation, it is fairly easy to describe various sections of the global phase diagram; examples are shown in Figs. 3 and 5. Some of these aspects, in particular in the vicinity of the tricritical lines, will be taken up in a future paper.

ACKNOWLEDGMENTS

We are grateful to A. N. Berker and S. Ostlund for a number of useful suggestions and other assistance with our calculations. Our research was supported by the NSF through Grant No. DMR 78-20394 to Carnegie-Mellon University and through the Materials Science Center at Cornell University.

APPENDIX A: THE INVARIANT MANIFOLD $\bar{a} = \bar{b}, \bar{c} = 0$ ($J = H_3 = 0$)

Griffiths²⁰ and Bernasconi and Rys²⁵ have shown that the manifold $\bar{a} = \bar{b}, \bar{c} = 0$ for the three component model (or $J = H_3 = 0$ in the spin representation) can be mapped by an exact transformation onto the spin- $\frac{1}{2}$ Ising model, and thus the corresponding phase diagram is known exactly for a square or triangular lattice. Specifically, for a square lattice there is a line of critical points at

$$2 \cosh \bar{\mu}_a = \exp \bar{\mu}_c ; T = [8 \ln(1 + \sqrt{2})]^{-1} \quad (\text{A1})$$

(where we adopt the convention that $\bar{\mu}_a = -\bar{\mu}_b$) and a two-phase coexistence surface at smaller values of T .

The Migdal-Kadanoff scheme used in this paper maps this manifold onto itself and generates a critical line with two segments, governed by the fixed points $\langle B \rangle_{\alpha\gamma}$ and $\langle B \rangle_{\beta\gamma}$, meeting at the fixed point $\langle B \rangle_{\gamma}^0$. The coexistence surface is governed by the fixed points $\langle A^2 \rangle_{\alpha}$, $\langle A^2 \rangle_{\beta}$, and $\langle A^2 \rangle_{\gamma}^0$, and there are additional high-temperature fixed points whose properties are unimportant for critical phenomena. The recursion relations predict a phase diagram whose topology is the same as the exact result (previous paragraph). However, in some other respects the renormalization-group scheme shows significant differences. The exponents associated with $\langle B \rangle_{\gamma}^0$ are not exactly equal to those at $\langle B \rangle_{\alpha\gamma}$ and $\langle B \rangle_{\beta\gamma}$, which means that $\langle B \rangle_{\gamma}^0$ is singled out as a special point on the critical line. Indeed, the critical line exhibits a (rather small) cusp, Fig. 6, at $\langle B \rangle_{\gamma}^0$, whereas the exact result, (A1), is a smooth curve. For the recursion relations to produce a smooth curve of critical points belonging to the same universality class, it would be necessary to have the "extra" positive exponent (relevant eigenvalue) for $\langle B \rangle_{\gamma}^0$, ν_1 in Table III, equal to $\frac{1}{2}\nu_4$, as well as the other positive exponents identical to their values for $\langle B \rangle_{\alpha\gamma}$ and $\langle B \rangle_{\beta\gamma}$.

On the other hand, if we regard the renormalization scheme as an exactly soluble model on a special lattice,¹⁴ rather than an approximation for the square lattice, $\langle B \rangle_{\gamma}^0$ corresponds to some sort of multicritical point with a codimension of 3, and of course the same is true of $\langle B \rangle_{\alpha}^0$ and $\langle B \rangle_{\beta}^0$. The argument referred to in the first paragraph fails for the special lat-

tice because the latter lacks the necessary translational invariance.

The alternative recursion relations proposed by Emery and Swendsen¹⁵ also leave the manifold $J = H_3 = 0$ invariant, and produce a line of critical fixed points at

$$2 \cosh \bar{\mu}_a = \exp \bar{\mu}_c ; \quad T = 0.8205/q , \quad (\text{A2})$$

together with a line of discontinuity or first-order fixed points at $T = 0$, and a surface of fixed points at $T = \infty$. The phase diagram in this scheme is in better agreement with the exact results in that the critical (fixed) point at $\bar{\mu}_a = 0$ ($H = 0$) has the same properties as all the others. (Some disadvantages of this recursion scheme are that its "magnetic" exponent is significantly smaller than the exact value, and there is no exponent equal to d at any of the discontinuity fixed points.)

APPENDIX B: CROSSOVER TO THE SATELLITE FIXED POINTS

Our Migdal-Kadanoff recursion relations predict flows from the symmetrical fixed point $\langle B \rangle_{\gamma}$ to its off-symmetry satellites, $\langle B \rangle_{\gamma\alpha}$ and $\langle B \rangle_{\gamma\beta}$, but there is no corresponding crossover between two different critical regimes, and indeed there is a sense in which the three fixed points can be considered to be a single point. The same comment applies to $\langle BA \rangle_{\gamma}$ and its satellites $\langle BA \rangle_{\gamma\alpha}$ and $\langle BA \rangle_{\gamma\beta}$.

To see that this is the case, note that $\langle B \rangle_{\gamma}$, $\langle B \rangle_{\gamma\alpha}$, and $\langle B \rangle_{\gamma\beta}$ all occur at $\zeta_c = 0$ (Table II), which means that $\bar{\mu}_c$ in (2.2) is equal to $-\infty$. Thus the Boltzmann factor fixes the average of P_i^{γ} equal to zero for every i , as a consequence of which the energy, (2.2), and the corresponding free energy are independent of \bar{a} and \bar{b} . Since the renormalization-group flows from $\langle B \rangle_{\gamma}$ to $\langle B \rangle_{\gamma\alpha}$ keep all the parameters *except* for a and b fixed, it is no surprise that they leave the free energy unchanged and thus produce no change in critical behavior.

A similar analysis applies in the case of $\langle BA \rangle_{\gamma}$, $\langle BA \rangle_{\gamma\alpha}$, and $\langle BA \rangle_{\gamma\beta}$, which occur at \bar{a} and $\bar{b} = \infty$ (Table II), with flows between them corresponding to a variation of $\bar{a} - \bar{b}$ with all other parameters fixed. The Boltzmann factor, see (2.2), then implies the vanishing of the averages of all nearest-neighbor products of the form $P_i^{\beta} P_j^{\gamma}$ and $P_i^{\alpha} P_j^{\gamma}$, as a consequence of which a variation of $\bar{a} - \bar{b}$ changes neither the energy nor the free energy. This fact is correctly reflected in the renormalization-group formula for the free energy.

A similar "Ising-to-Ising" crossover has been found in renormalization-group studies based on the $\epsilon = 4 - d$ expansion²⁶ and in a real-space renormalization-group calculation.²⁷

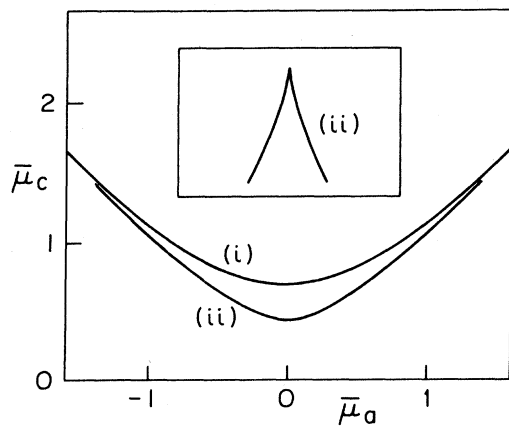


FIG. 6. Locus of critical points for $\bar{a} = \bar{b}, \bar{c} = 0$ projected along the T axis on the $\bar{\mu}_a, \bar{\mu}_c$ plane: (i) the exact result and (ii) Migdal-Kadanoff scheme. The inset shows (ii) in the immediate vicinity of $\bar{\mu}_a = 0$ with the horizontal and vertical axes magnified by factors of 3×10^4 and 3×10^6 , respectively.

- ¹D. Furman, S. Dattagupta, and R. B. Griffiths, Phys. Rev. B 15, 441 (1977). The reader is referred to the bibliography in this paper for references to earlier work on the mean-field theory.
- ²M. Blume, V. J. Emery, and R. B. Griffiths, Phys. Rev. A 4, 1071 (1971).
- ³R. B. Griffiths, Phys. Rev. B 12, 345 (1975).
- ⁴J. P. Straley and M. E. Fisher, J. Phys. A 6, 1310 (1973); R. J. Baxter, J. Phys. C 6, L445 (1973).
- ⁵L. D. Landau and E. M. Lifshitz, *Statistical Physics*, 2nd ed. (Pergamon, London, 1969), Chap. XIV.
- ⁶A. N. Berker and M. Wortis, Phys. Rev. B 14, 4946 (1976).
- ⁷T. W. Burkhardt, Phys. Rev. B 14, 1196 (1976); T. W. Burkhardt and H. J. Knops, *ibid.* 5, 1602 (1977).
- ⁸G. D. Mahan and S. M. Gurrin, Phys. Rev. B 17, 4411 (1978).
- ⁹J. Adler, A. Aharony, and J. Oitmaa, J. Phys. A 11, 963 (1978).
- ¹⁰S. Krinsky and D. Furman, Phys. Rev. Lett. 32, 731 (1974); Phys. Rev. B 11, 2602 (1975).
- ¹¹S. Sarbach and M. E. Fisher, Phys. Rev. B 18, 2350 (1978); 20, 2797 (1979).
- ¹²A. A. Migdal, Sov. Phys. JETP 42, 743 (1976) [Zh. Eksp. Teor. Fiz. 69, 1457 (1975)]; L. P. Kadanoff, Ann. Phys. (N.Y.) 100, 359 (1976). Note that in the latter the approximate renormalization group is defined in a way which maps an initially isotropic lattice onto an anisotropic lattice: here we employ a modification of the scheme for which isotropy is preserved.
- ¹³J. V. José, L. P. Kadanoff, S. Kirkpatrick, and D. R. Nelson, Phys. Rev. B 16, 1217 (1977), Appendix B.
- ¹⁴A. N. Berker and S. Ostlund, J. Phys. C 12, 4961 (1979).
- ¹⁵V. J. Emery and R. H. Swendsen, Phys. Lett. A 64, 325 (1977).
- ¹⁶L. Onsager, Phys. Rev. 65, 117 (1944).
- ¹⁷M. P. M. den Nijs, J. Phys. A 12, 1857 (1979); B. Nienhuis, E. K. Riedel, and M. Schick, J. Phys. A 13, L189 (1980).
- ¹⁸B. Nienhuis and M. Nauenberg, Phys. Rev. Lett. 35, 477 (1975).
- ¹⁹B. Nienhuis, A. N. Berker, E. K. Riedel, and M. Schick, Phys. Rev. Lett. 43, 737 (1979); B. Nienhuis, E. K. Riedel, and M. Schick, J. Phys. A 13, L31 (1980).
- ²⁰R. B. Griffiths, Physica (Utrecht) 33, 689 (1967).
- ²¹R. B. Potts, Proc. Cambridge Philos. Soc. 48, 106 (1952).
- ²²B. L. Arora and D. P. Landau, in *Magnetism and Magnetic Materials—1972 (Denver)*, edited by C. D. Graham and J. J. Rhyne, AIP Conf. Proc. No. 10 (AIP, New York, 1973), p. 870.
- ²³A. K. Jain and D. P. Landau as reported in Ref. 7.
- ²⁴This can be inferred from the discussion in Ref. 3 and R. B. Griffiths, J. Chem. Phys. 60, 195 (1974).
- ²⁵J. Bernasconi and F. Rys, Phys. Rev. B 4, 3045 (1971).
- ²⁶D. R. Nelson and M. E. Fisher, Phys. Rev. B 11, 1030 (1974).
- ²⁷B. Nienhuis and M. Nauenberg, Phys. Rev. B 13, 2021 (1976).